

Lymphokine-Activated Killer T-Cell-Originated Protein Kinase Phosphorylation of Histone H2AX Prevents Arsenite-Induced Apoptosis in RPMI7951 Melanoma Cells

Tatyana A. Zykova,¹ Feng Zhu,¹ Chengrong Lu,¹ LeeAnn Higgins,² Yasuaki Tatsumi,¹ Yasuhito Abe,³ Ann M. Bode,¹ and Zigang Dong¹

Abstract Purpose: Arsenic is a valuable therapeutic tool in cancer treatment. Lymphokine-activated killer T-cell-originated protein kinase (TOPK) is highly expressed in cancer cells, but its specific function is still unknown. We investigated the role of TOPK in arsenic-induced apoptosis in RPMI7951 human melanoma cells.

Experimental Design: Expression of TOPK was evaluated in different melanoma cell lines, and liquid chromatography-tandem mass spectrometry analysis was used to identify proteins binding with TOPK. Immunofluorescence, Western blot, and flow cytometry were used to assess the effect of arsenic on TOPK, histone H2AX, and apoptosis in RPMI7951 cells.

Results: Melanoma cell lines expressing high levels of TOPK were more resistant to arsenite (As^{3+})-induced apoptosis. As^{3+} treatment induced phosphorylation of TOPK and histone H2AX in RPMI7951 human melanoma cells. Liquid chromatography-tandem mass spectrometry results indicated that TOPK could bind with histone H2AX, and *in vitro* and *in vivo* assays confirmed that TOPK binds with and phosphorylates histone H2AX. As^{3+} treatment caused phosphorylation of TOPK, which colocalized with phosphorylated histone H2AX in the nucleus. TOPK small interfering RNA cells exhibited a decreased phosphorylation of histone H2AX with As^{3+} treatment. As^{3+} -induced apoptosis was decreased in H2AX^{-/-} cells but increased in TOPK small interfering RNA cells.

Conclusions: TOPK binds with histone H2AX and inhibits As^{3+} -induced apoptosis through phosphorylation of histone H2AX. Melanoma cell lines with high levels of TOPK are more resistant to As^{3+} -induced apoptosis. Therefore, inhibition of TOPK activity combined with As^{3+} treatment may be helpful in the treatment of melanomas.

Lymphokine-activated killer T-cell-originated protein kinase (TOPK) is a novel mitotic protein kinase that is highly expressed only in various cancers, such as leukemia, myeloma, and lymphoma, and its expression has been correlated with the malignant potential of these tumors (1–4). TOPK is phosphorylated and active only during mitosis (2) and has been shown to phosphorylate the p38 mitogen-activated protein kinase but not extracellular signal-regulated kinases or c-Jun

NH₂-terminal kinases (JNK; ref. 1). Recent reports showed that TOPK is up-regulated in murine myeloma cells by an interleukin-6-mediated protein-protein interaction between TOPK and Raf-A (4, 5). In addition, TOPK is involved in cell cycle regulation and can be a substrate of cdc2/cyclin B (2, 6). TOPK expression has also been shown to be up-regulated during the G₂ to M phase transition, where the cdc2/cyclin B complex plays an important role (6). Thr⁹ is an important phosphorylation site of TOPK because, when Thr⁹ was substituted to Ala, the binding ability of TOPK to cdc2/cyclin B was decreased (6). The cell cycle-specific transcription factors E2F and cyclic AMP-responsive element binding protein/activating transcription factor are critical regulators of TOPK expression during growth arrest in leukemia cells (7). Thus, TOPK may be a potential target for chemotherapeutic or chemopreventive compounds.

The effectiveness of many therapeutic approaches, including γ -irradiation and chemotherapeutic drug treatment, has been proposed to be associated with the reactivation of apoptosis in cancer cells. Arsenic is a paradoxical compound that induces global changes in gene expression and cell signal transduction pathways in different types of cells (8, 9). Dose-dependent effects of arsenic in a tissue-specific manner have enabled arsenic to be used for the effective treatment of certain types of cancers, including leukemia and myeloma, through its

Authors' Affiliations: ¹Hormel Institute, University of Minnesota, Austin, Minnesota; ²Department of Biochemistry, Molecular Biology and Biophysics, St. Paul, Minnesota; and ³Department of Pathology, Division of Molecular Pathology, Ehime University School of Medicine, Tohon, Ehime, Japan
Received 2/20/06; revised 4/24/06; accepted 9/13/06.

Grant support: Hormel Foundation and NIH grants CA77646, CA111356, and CA111536.

The costs of publication of this article were defrayed in part by the payment of page charges. This article must therefore be hereby marked *advertisement* in accordance with 18 U.S.C. Section 1734 solely to indicate this fact.

Note: T.A. Zykova and F. Zhu contributed equally to this work.

The University of Minnesota is an equal opportunity educator and employer.

Requests for reprints: Zigang Dong, Hormel Institute, University of Minnesota, 801 16th Avenue Northeast, Austin, MN 55912. Phone: 507-437-9600; Fax: 507-437-9606; E-mail: zgdong@hi.umn.edu.

©2006 American Association for Cancer Research.
doi:10.1158/1078-0432.CCR-06-0410

induction of apoptosis (10, 11). Arsenic treatment has been shown to induce the up-regulation of cyclin B1 and activates the cdc2/cyclin B1 complex in mitotic cells (12) and therefore could have an effect on TOPK and its potential binding partners.

Melanomas develop through well-defined morphologic and histologic stages that involve the loss of cell proliferation control, the acquisition of invasiveness, and, ultimately, the acquisition of metastatic potential (13). Melanoma cells generally express chromosome instability during their development (14). Histone H2AX has been shown to prevent aberrant repair of both programmed and general DNA breakage (15). H2AX deficiency decreases genomic stability and increases tumor susceptibility of normal cells and tissues (16). In addition, a lack of histone H2AX causes genomic instability in mice (17). Here, we have investigated a functional relationship and interaction of TOPK and histone H2AX in mediating arsenite (As^{3+})-induced apoptosis in melanoma cells. Results indicated that As^{3+} -induced phosphorylation of TOPK and TOPK directly phosphorylated histone H2AX, resulting in the inhibition of As^{3+} -induced apoptosis in RPMI7951 melanoma cells. This suggested that TOPK could be a potential target for chemotherapeutic treatment of melanomas.

Materials and Methods

Reagents and antibodies. As^{3+} and anti- β -actin were from Sigma (St. Louis, MO); NE-PER Nuclear and Cytoplasmic Extraction Reagents were from Pierce Biotechnology (Rockville, IL). Stock solutions of As^{3+} (10 mmol/L) in 0.1% DMSO were stored at $-20^{\circ}C$. PDZ-binding kinase/TOPK, phosphorylated PDZ-binding kinase/TOPK (Thr⁹) antibodies, and active glutathione S-transferase-TOPK were from Cell Signaling Technology, Inc. (Beverly, MA); anti-histone H2AX, anti-phosphorylated H2AX, and histone H2AX (recombinant protein expressed in *Escherichia coli*) were from Upstate Biotechnology, Inc. (Lake Placid, NY); anti-hemagglutinin (HA) probe (F-7) was from Santa Cruz Biotechnology (Santa Cruz, CA).

Cell culture. SK-MEL5 and SK-MEL28 human malignant melanoma and SK-MEL31 and RPMI7951 human malignant melanoma epithelial-like cell lines were from the American Type Culture Collection (Manassas, VA). Human melanoma cell lines were cultured in MEM containing 10% fetal bovine serum (FBS; 15% FBS for SK-MEL31), 2 mmol/L L-glutamine, and 25 μ g/mL gentamicin, 0.1 mmol/L nonessential amino acids, and 1 mmol/L sodium pyruvate (SK-MEL31 also required 1.5 g/L sodium bicarbonate) at $37^{\circ}C$ in humidified air with 5% CO_2 . Mouse epidermal JB6 promotion-sensitive Cl41 cells were cultured in MEM containing 5% FBS, 2 mmol/L L-glutamine, and 25 μ g/mL gentamicin at $37^{\circ}C$ in humidified air with 5% CO_2 . H2AX^{+/+} and H2AX^{-/-} cell lines were a gift from Dr. Andre Nussenzweig (Experimental Immunology Branch, National Cancer Institute, NIH, Bethesda, MD) and were cultured in DMEM supplemented with 10% FBS, 2 mmol/L L-glutamine, and 25 μ g/mL gentamicin at $37^{\circ}C$ in humidified air with 5% CO_2 .

Generation of the TOPK-overexpressing cell line. pc-DNA3, pcDNA3-HA-TOPK, or mutant pcDNA3-HA-TOPK-T9A (gifts from Dr. J. Abe, Department of Pathology, Division of Molecular Pathology, Ehime University School of Medicine, Toh-on, Ehime, Japan; ref. 6) was transfected into JB6 Cl41 cells using SuperFect (Qiagen, Valencia, CA). Transfected cells were selected in MEM containing 5% FBS and G418 (800 μ g/mL) for 2 weeks. Stable cell lines were maintained in MEM containing 5% FBS and 200 μ g/mL G418.

Small interfering RNA preparation and vector construction. Two pairs of hairpin small interfering RNA (siRNA) oligonucleotides, containing

*Bam*HI and *Hind*III sites, were designed as described previously (18). Hairpin siRNA template oligonucleotides were chemically synthesized, deprotected, and gel purified by Sigma-Genosys (Woodlands, TX). The TOPK siRNA sequence target sequences were aligned to the genome database in a BLAST search to ensure sequences without significant homology to other genes. The sense siRNA template sequence for TOPK was 5'-GATCCGAGGTTGTCTCATTCTCCTTCAAGAGAGGAGAATGAGACAAACCTCTTTTTGGAAA-3' and the antisense siRNA template sequence was 5'-AGCTTTTCCAAAAAGAGGTTGTCTCATTCTCCTTGAAGGAGAATGAGACAAACCTCG-3'. The sense and antisense oligonucleotides were annealed and cloned into the pSilencer 3.1-H1 neo vector (Ambion, Austin, TX) at the *Bam*HI and *Hind*III sites as described by the manufacturer. A scrambled siRNA with a sequence lacking significant homology to the mouse, human, or rat genome database was used as the control or mock siRNA. The resulting pSilencer 3.1-H1-siRNA plasmids were transfected into RPMI7951 cells, and the stable cell lines were obtained by G418 screening. These TOPK siRNA cell lines were cultured in MEM supplemented with 10% FBS, 2 mmol/L L-glutamine, 25 μ g/mL gentamicin, 0.1 mmol/L nonessential amino acids, 1 mmol/L sodium pyruvate, and 200 μ g/mL G418.

Identification of proteins binding with TOPK by liquid chromatography-tandem mass spectrometry analysis. The *topk* gene was amplified by PCR and then cloned into pET-46 using a pET-46 Ek/LIC kit (Novagen, Inc., Madison, WI). His-TOPK was purified from BL21 (DE3) cells (Novagen). His-TOPK (0.5 mg) was used for binding with 400 μ L Ni-NTA agarose beads (Qiagen, Hilden, Germany). Then, a lysate (10 mg) of RPMI7951 cells was incubated with His-TOPK beads at $4^{\circ}C$ overnight. The TOPK-binding proteins were eluted with 50% acetonitrile (Fisher Biotech, Fair Lawn, NJ). Approximately 12 μ g of protein eluted from the His-TOPK beads were digested in solution with sequencing grade-modified trypsin (Promega, Madison, WI) according to the manufacturer's protocol. The sample was purified using a C18 SepPak cartridge (Waters Institute, Milford, MA) according to the manufacturer's directions and then speed vacuumed to dryness. The peptide mixture was reconstituted with loading buffer (98:2, H_2O /acetonitrile, 0.1% formic acid) and analyzed by capillary liquid chromatography-tandem mass spectrometry (LC-MS/MS; refs. 19, 20). Product ion mass spectra were searched against the nonredundant database⁴ of National Center for Biotechnology Information (April 20, 2005; total 1,182,676 protein sequences), interpreted using the Pro ID version 1.1 software (Applied Biosystems, Inc., Foster City, CA), which used the Interrogator algorithm for scoring peptide/protein candidates (21), and results were verified by manual interpretation.

SDS-PAGE and Western blotting. Cell lines (7×10^5) were cultured in their respective medium for 12 to 15 hours in 10-cm-diameter dishes to 70% to 80% confluence. Cells were treated with As^{3+} and harvested after 24 hours with 200 μ L of radioimmunoprecipitation assay buffer (1 \times PBS, 1% NP40, 0.5% sodium deoxycholate, 0.1% SDS, 1 mmol/L Na_3VO_4 , 1 mmol/L aprotinin, 1 mmol/L phenylmethylsulfonyl fluoride). The quantity of protein was determined by the Bradford method (22). The samples (30-50 μ g protein) with 5 \times SDS were loaded into 10% to 15% SDS polyacrylamide gel for electrophoresis and subsequently transferred onto an Immobilon-P transfer membrane (Millipore, Chelmsford, MA). Antibody-bound proteins were detected by chemiluminescence (Enhanced Chemifluorescence, Amersham Pharmacia Biotech, Piscataway, NJ) and analyzed using the Storm 840 Scanner (Molecular Dynamics, Sunnyvale, CA). Untreated cell samples were used as negative controls.

In vitro kinase assays. Samples containing recombinant histone H2AX expressed in *E. coli* were incubated at $30^{\circ}C$ for 30 minutes with active glutathione S-transferase-TOPK in 10 \times kinase buffer A [50 mmol/L Tris-HCl (pH 7.5), 10 mmol/L $MgCl_2$, 1 mmol/L EGTA, 1 mmol/L DTT, 0.01% Brij 35; Cell Signaling Technology] containing 200 μ mol/L ATP. The reactions were stopped by adding 5 \times SDS sample

⁴ <http://www.ncbi.nlm.nih.gov>.

buffer. Then, phosphorylation of H2AX (Ser¹³⁹) was analyzed by Western blot using a phosphorylated H2AX (Ser¹³⁹) antibody. Phosphorylation of histone H2AX by JNK1 was used as a positive control. For some experiments, equal protein loading was verified by silver staining for histone H2AX.

Immunofluorescence assay. To determine the translocation ability of phosphorylated TOPK and phosphorylated H2AX, RPMI7951 melanoma cells (5×10^5) treated or not treated with 2.5 $\mu\text{mol/L}$ As³⁺ were incubated for 24 hours. Cells were fixed in 4% paraformaldehyde and incubated with anti-phosphorylated TOPK and anti-phosphorylated H2AX and then with either FITC-conjugated secondary antibody or Texas red-conjugated secondary antibody (Invitrogen, Carlsbad, CA). Samples were analyzed with a fluorescence microscope system (Leica, Mannheim, Germany).

Isolation of histone H2AX. Histones were extracted from As³⁺-treated cells by disrupting cells with NETN buffer [150 mmol/L NaCl, 1 mmol/L EDTA, 20 mmol/L Tris (pH 8.0), 0.5% nonionic detergent Igepal CA630 (NP40); Sigma]. The insoluble fraction was pelleted for 5 minutes in a microcentrifuge (8,400 rpm). Nuclei were extracted with 0.1 N HCl to isolate total histones. Samples were precipitated with 1 mol/L Tris-HCl (pH 8.0) and then resuspended in double-distilled water (23).

Flow cytometry analysis. Apoptosis induced by As³⁺ was determined using the Annexin V-FITC Apoptosis Detection kit (Medical & Biological Laboratories, Nagoya, Japan) according to the protocol provided. Briefly, cells were trypsinized, washed once with MEM containing serum, and incubated with Annexin V-conjugated FITC. Apoptosis was analyzed using a flow cytometer (FACSCalibur, Becton Dickinson, Franklin Lakes, NJ).

Statistical analysis. Comparisons were made using one-way ANOVA, and data are expressed as mean \pm SD of three to four independent experiments. Differences were considered significant with $P < 0.05$.

Results

TOPK expression in human melanoma cell lines. TOPK is expressed in a wide range of cancers, including leukemia, myeloma, and lymphoma (1–4, 7). However, the expression of TOPK in melanoma cells is yet to be determined. Thus the expression of TOPK was compared in the mouse epidermal JB6 Cl41 skin cell line and in four different human malignant melanoma cell lines, SK-MEL28, SK-MEL31, SK-MEL5, and RPMI7951, which are routinely used in our laboratory. Results indicated that the expression of TOPK in the SK-MEL28 and RPMI7951 cell lines was highest compared with SK-MEL31, SK-MEL5, or JB6 Cl41 cells (Fig. 1). Based on these results, we chose the RPMI7951 melanoma cell line to study TOPK function and to identify potential binding partners.

Identification of TOPK-binding partners by LC-MS/MS. First, a His-TOPK protein was generated and was found to bind strongly with Ni-NTA agarose beads. His-TOPK was confirmed to remain bound to the beads even after elution with 50% acetonitrile (data not shown). Therefore, His-TOPK-Ni-NTA agarose (His-TOPK) beads could be used for immobilizing TOPK-binding proteins for subsequent identification. RPMI7951 cell lysate was incubated with Ni-NTA agarose beads as a negative control (Fig. 2A, lane 1) or Ni-NTA-His-TOPK beads (Fig. 2A, lane 2). After washing with PBS, proteins binding with His-TOPK beads were visualized with silver staining after elution with 50% acetonitrile (Fig. 2A). LC-MS/MS analysis (24) identified 26 individual proteins that could bind with TOPK (data not shown). A fragment composed of 19 amino acids, VTIAQGGVLPNIQAVLLPK, was identified with

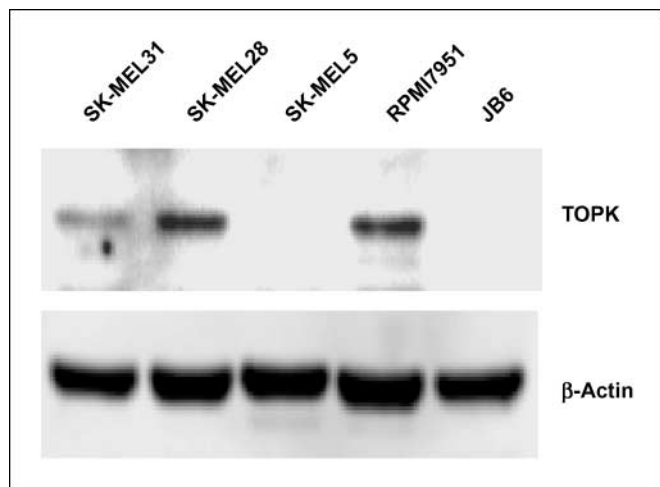


Fig. 1. TOPK expression in several cell lines. Mouse skin JB6 Cl41 cells and several different human melanoma cell lines were screened by Western blot to determine the total protein expression level of endogenous nonphosphorylated TOPK. β -Actin was used to verify equal protein loading. These data are representative of at least three independent experiments.

a Pro ID confidence of 99% as a peptide from the family of H2A proteins (Fig. 2B). The human genome contains 16 genes that encode for H2A peptides classified as H2A variants (25). The identified peptide sequence was 100% homologous to the sequences of 12 genes of the 16 H2A histone family members, including the important H2A variant, H2AX. A role for H2AX phosphorylation has been shown in DNA repair, cell cycle checkpoint regulation, regulation of gene recombination events, and tumor suppression (26). The LC-MS/MS result suggested that TOPK could bind with histone H2AX. Thus, we focused on elucidating the function and the physiologic significance of the interaction of TOPK and histone H2AX.

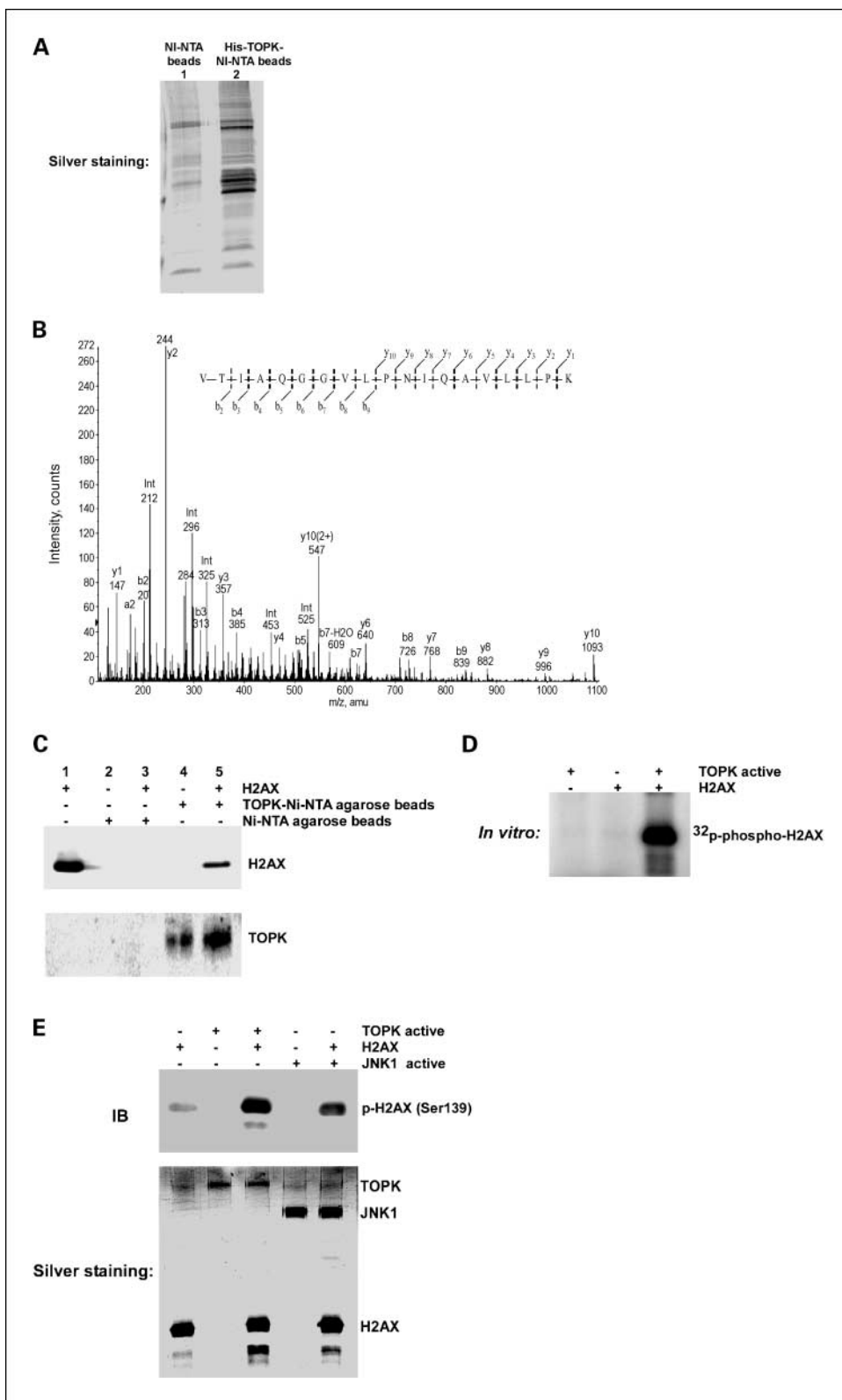
TOPK binds with and phosphorylates histone H2AX in vitro. Histone H2AX was incubated with Ni-NTA agarose beads (as a negative control) or His-TOPK-Ni-NTA agarose beads at 30°C for 30 minutes. The binding interaction was analyzed by Western blot using an H2AX antibody. Results confirmed that TOPK binds with histone H2AX (Fig. 2C). Because TOPK is a kinase, we next determined whether TOPK can phosphorylate histone H2AX by using histone H2AX as substrate for active TOPK. The phosphorylation was visualized by autoradiography in the presence of [γ -³²P]ATP (Fig. 2D) or by a phosphorylated H2AX (Ser¹³⁹) antibody (Fig. 2E). Phosphorylation of H2AX by JNK1 was used as positive control (27). These results strongly indicated that TOPK binds with and phosphorylates H2AX at Ser¹³⁹ *in vitro*. Silver staining of H2AX, TOPK, and JNK1 was used as an internal control to verify equal protein loading.

As³⁺ induces phosphorylation of TOPK and H2AX in RPMI7951 melanoma cells. As³⁺ is a toxin with multiple effects in animal and human populations. Low concentration doses of As³⁺ have been reported to induce apoptosis of human melanoma cells (10, 11). The effect of As³⁺ on TOPK (Thr⁹) or H2AX (Ser¹³⁹) phosphorylation in RPMI7951 melanoma cells was investigated herein by using Western blot analysis. Results indicated that a strong phosphorylation of TOPK (Thr⁹) and H2AX (Ser¹³⁹) was induced in a dose-dependent manner following a 24-hour As³⁺ treatment of RPMI7951 cells (Fig. 3, top and middle top).

For further experiments, cells were treated with 2.5 μmol/L As³⁺ and harvested 24 hours after treatment. No change in the nonphosphorylated levels of TOPK or H2AX expression was observed in these cell lines under these conditions with As³⁺ treatment (Fig. 3, bottom and middle bottom).

Phosphorylated TOPK and phosphorylated H2AX colocalize in the nucleus after As³⁺ treatment. Yih et al. (28) previously reported that phosphorylated H2AX was clearly detectable in the interface nuclei of CGL-2 cells treated for 24 hours with 2 μmol/L As³⁺. In the present study, RPMI7951 cells were

Fig. 2. TOPK binds with and phosphorylates histone H2AX *in vitro*. **A**, TOPK-binding proteins visualized by silver staining. Lane 1, silver staining of gel showing RPMI7951 cell lysate binding with Ni-NTA agarose beads; lane 2, silver staining of gel showing RPMI7951 cell lysate binding with His-TOPK-Ni-NTA agarose beads. **B**, tandem mass spectrum of the VTIAQGGVLPNIQAVLLPK peptide. The gene sequence of this peptide was found to be 100% homologous to the sequences of 12 genes of the 16 H2A histone family members, including histone H2AX. The error in the experimental peptide MW (1930.140) was within 11 ppm of the theoretical MW. Diagnostic b-type and y-type fragment ions are labeled with the value and the ion type according to the fragment ion nomenclature of Biemann (24). The amino acid sequence is displayed above and below the spectrum. The experimentally measured y and b ions are written above and below the sequence, respectively. **C**, confirmation of the binding of TOPK with histone H2AX *in vitro* using His-TOPK-Ni-NTA agarose beads. Histone H2AX was incubated with Ni-NTA agarose beads (as control, lane 3) or His-TOPK-Ni-NTA agarose beads (lane 5) at 30°C for 30 minutes. Their binding interaction was analyzed by Western blot using an H2AX antibody. H2AX only (lane 1), Ni-NTA agarose beads only (lane 2), and His-TOPK-Ni-NTA agarose beads only (lane 4) were used as controls. Bottom, the total levels of TOPK served to confirm the presence of TOPK bound to the beads. **D**, *in vitro* kinase assay to determine the ability of TOPK to phosphorylate histone H2AX visualized by autoradiography in the presence of [³²P]ATP. **E**, *in vitro* kinase assay to determine the ability of TOPK to phosphorylate histone H2AX visualized by Western blot using a phosphorylated H2AX (p-H2AX; Ser¹³⁹) antibody. The binding of JNK1 with H2AX was used as a positive control (unpublished data), and equal protein loading was verified by silver staining for H2AX. These data are representative of at least three independent experiments.



treated with 2.5 $\mu\text{mol/L}$ As^{3+} for 24 hours and then cytoplasmic and nuclear proteins were extracted and TOPK and phosphorylated TOPK were detected by Western blot (Fig. 4A). The results indicated that TOPK is located mostly in the cytoplasm with very little protein in the nucleus in the absence of As^{3+} treatment (Fig. 4A). TOPK localization to the nucleus increased dramatically with As^{3+} treatment (Fig. 4A, top), and phosphorylated TOPK was located only in the nucleus (Fig. 4A, bottom). Immunocytofluorescence analysis was used to further examine the nuclear localization and interaction of TOPK and histone H2AX (Fig. 4B). Results indicated that phosphorylated TOPK (green) and phosphorylated H2AX (red) were both localized in the nucleus after As^{3+} treatment (Fig. 4B, top and middle right). The merged result confirmed that TOPK colocalized with histone H2AX in the nucleus with As^{3+} treatment (Fig. 4B, bottom right).

TOPK siRNA-transfected cells inhibit the phosphorylation of histone H2AX. RPMI7951 cells were transfected with pSilencer 3.1-H1-topk-siRNA and selected by G418. The expression of TOPK was verified by Western blot using anti-TOPK. Results indicated that, in control siRNA mock-transfected cells, As^{3+} induced phosphorylation of TOPK (Thr⁹) and H2AX (Ser¹³⁹; Fig. 5A). On the other hand, As^{3+} -induced phosphorylation of histone H2AX (Ser¹³⁹), TOPK (Thr⁹), and nonphosphorylated TOPK was dramatically decreased in TOPK siRNA-transfected cells (Fig. 5A). The expression of total H2AX or β -actin was not different between these cell lines (Fig. 5A, bottom and middle

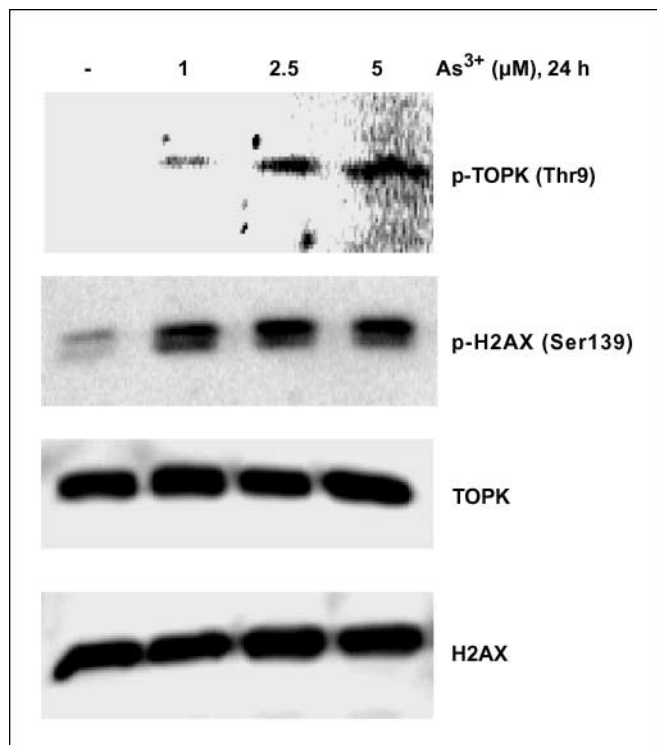


Fig. 3. Dose-dependent phosphorylation of TOPK (Thr⁹) and H2AX (Ser¹³⁹) is induced in As^{3+} -treated cells. RPMI7951 cells were harvested 24 hours after treatment with different doses of As^{3+} . TOPK and H2AX proteins in the cell lysate were separated by 10% or 15% SDS-PAGE, respectively, followed by Western blot analysis with specific antibodies against phosphorylation of TOPK at Thr⁹ and H2AX at Ser¹³⁹ or against nonphosphorylated TOPK or H2AX. Untreated samples served as negative controls. Total TOPK and H2AX were used to verify equal protein loading. These data are representative of at least three independent experiments.

bottom). Thus, these data indicated that TOPK is required for mediating As^{3+} -stimulated phosphorylation of H2AX at Ser¹³⁹.

Phosphorylation of histone H2AX is associated with inhibition of As^{3+} -induced apoptosis. H2AX^{+/+} and H2AX^{-/-} cell lines were treated for 24 hours with 2.5 $\mu\text{mol/L}$ As^{3+} , and phosphorylation of histone H2AX (Ser¹³⁹) and total histone H2AX was determined by Western blot analysis. As expected, the H2AX^{-/-} cell line displayed a markedly reduced expression and phosphorylation of histone H2AX compared with the H2AX^{+/+} cells (Fig. 5B). However, As^{3+} -induced phosphorylation of TOPK and the expression of total histone H3 or TOPK were similar in the two cell lines (Fig. 5B). Furthermore, early apoptosis was significantly less ($P < 0.0001$) following treatment with 2.5 $\mu\text{mol/L}$ As^{3+} at all time points in H2AX^{-/-} cells compared with H2AX^{+/+} cells (Fig. 5C, bottom right quadrants). This suggested that phosphorylation of H2AX protects cells against As^{3+} -induced apoptosis.

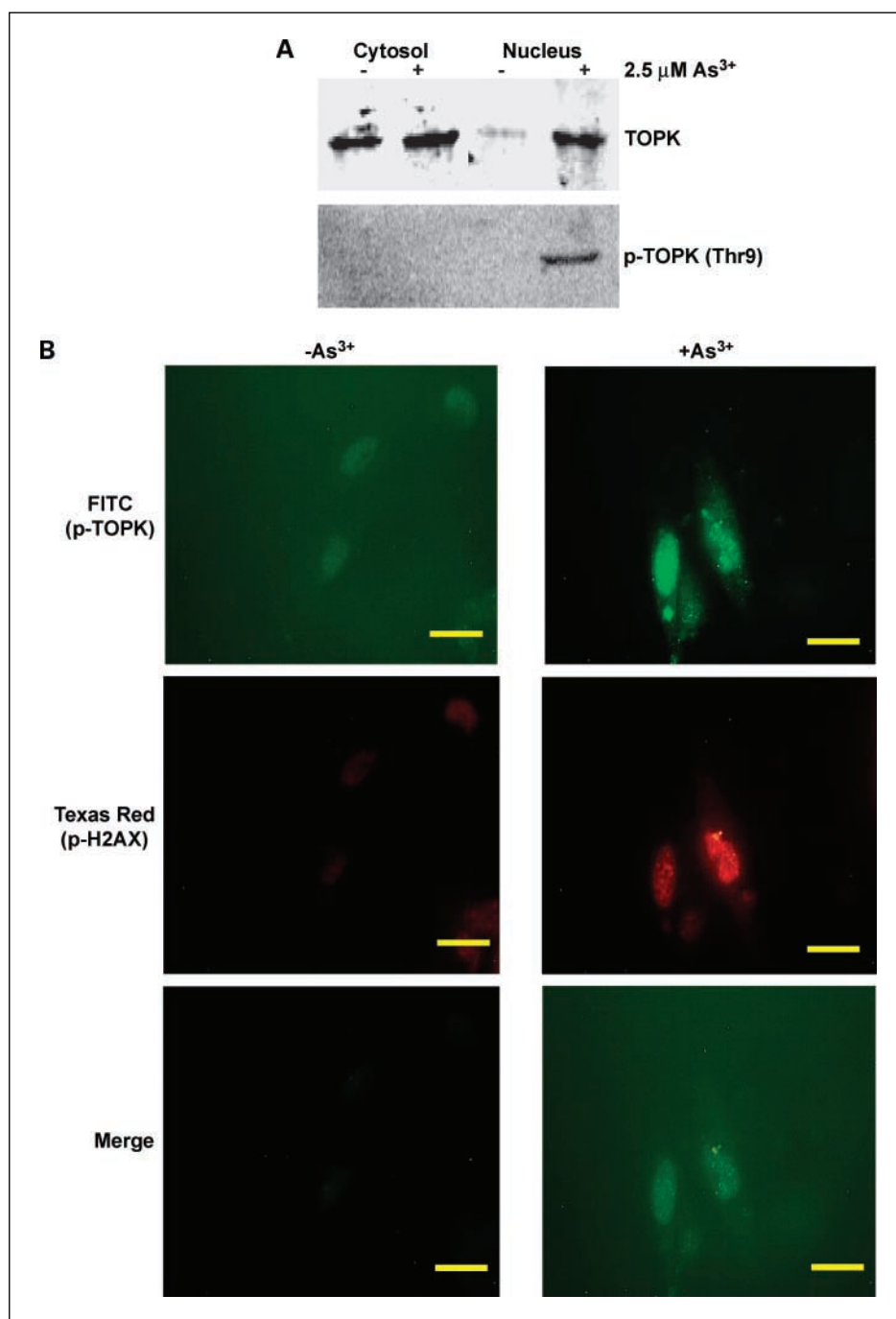
TOPK inhibits As^{3+} -induced apoptosis. Expression of TOPK was associated with decreased As^{3+} -induced apoptosis. At all times after As^{3+} treatment, a significant ($P < 0.0001$) increase in early apoptosis was observed in TOPK siRNA cells compared with control siRNA-transfected cells (Fig. 5D). This suggested that the absence of TOPK sensitizes cells to As^{3+} -induced apoptosis. Taken together, these results indicated that TOPK plays an important role in inhibiting As^{3+} -induced apoptosis through its phosphorylation of histone H2AX.

As^{3+} -induced apoptosis is dependent on TOPK status. We further confirmed these results by examining the effect of As^{3+} treatment on apoptosis in human melanoma cells, including SK-MEL28, SK-MEL31, SK-MEL5, and RPMI7951 cells, which have varying expression levels of TOPK. RPMI7951 and SK-MEL28 cells, which both express TOPK, showed very little induction of apoptosis by As^{3+} at all time points tested (Fig. 6A). In contrast, apoptosis was markedly induced in SK-MEL31 and SK-MEL5, which express low levels of TOPK (Fig. 6B). To further confirm that the expression level of TOPK has a major influence on whether As^{3+} can induce apoptosis, JB6 Cl41 cells, which do not express TOPK (see Fig. 1), were transfected with pcDNA3 mock vector (JB6/Vector), pcDNA3-HA-TOPK for overexpression of TOPK, or pcDNA3-HA-TOPK-T9A for overexpression of a mutant TOPK (Tyr⁹ replaced with alanine). Expression of these plasmids was verified by Western blot using a HA antibody (Fig. 6C). Induction of apoptosis by As^{3+} in JB6/Vector cells was ~60% after 72 hours and ~42% in JB6-pcDNA3-HA-TOPK-T9A cells (Fig. 6D). In contrast, very little apoptosis occurred in TOPK-overexpressing cells at any time point. This suggested that suppression of TOPK activity by the mutant TOPK-T9A cells almost totally restored the apoptotic response to As^{3+} . Overall, these results indicated that TOPK is critical in protecting against As^{3+} -induced apoptosis and thus could be an important target in As^{3+} treatment of cancers.

Discussion

TOPK is highly expressed in lymphoma cells, in myeloid leukemia cells, and in several other highly proliferative malignant cell lines derived from sarcomas, carcinomas, or myelomas of various tissue origins (3, 29). In the present study, we used LC-MS/MS analysis to confirm that His-TOPK could bind with histone H2AX. The *in vitro* kinase data indicated that TOPK directly interacted with and phosphorylated histone

Fig. 4. TOPK and histone H2AX colocalize in the nucleus. *A*, cytosolic and nuclear localization of total and phosphorylated TOPK in RPMI7951 cells after 24 hours of treatment with 2.5 $\mu\text{mol/L}$ As^{3+} . Cytosolic and nuclear proteins were extracted and separated by 10% SDS-PAGE followed by Western blot analysis with specific antibodies against phosphorylated (*p-TOPK*) and nonphosphorylated TOPK. *B*, nuclear colocalization of phosphorylated TOPK and phosphorylated H2AX. RPMI7951 cells were or were not treated with 2.5 $\mu\text{mol/L}$ As^{3+} for 24 hours. TOPK was visualized under a fluorescence microscope using a FITC-specific antibody (*top*), and histone H2AX was visualized (*middle*) using a Texas red – conjugated antibody. Pictures of As^{3+} -treated (*right*) and As^{3+} -untreated (*left*) cells represent exactly the same region for each, respectively, allowing the bottom pictures to show the merged staining result. Magnification, $\times 630$. Bar, 25 μm . These data are representative of at least three independent experiments.



H2AX. This is significant because H2AX has been designated as the histone guardian of the genome (26). Phosphorylation of H2AX has been suggested to have two important functions in DNA repair: to promote changes in the structural configuration of chromatin and to assist in chromatin binding of repair factors. These functions may or may not be related, but both are likely to be required for efficient synapses of broken chromosome ends (26, 30). Several reports have shown that As^{3+} can induce DNA damage (31, 32). Our laboratory has focused on the elucidation of mechanisms explaining how arsenic can act both as a carcinogen and as an effective chemotherapeutic agent (9, 33, 34). Accumulating data suggested that As^{3+} may

specifically induce apoptosis in certain types of tumor cells, including megakaryocytic leukemia cell lines, human breast cancer cells (32), and human myeloma cells (11, 34, 35). Furthermore, mitogen-activated protein kinases have been shown to have a very important role in mediating As^{3+} -induced apoptosis (36).

TOPK, a novel mitogen-activated protein kinase kinase-like protein kinase (6), is highly expressed in tumor cells but not in normal cells, and the function of this kinase is not clear. In this study, we showed that As^{3+} induced phosphorylation of both TOPK (Thr⁹) and histone H2AX (Ser¹³⁹) and that TOPK directly phosphorylated histone H2AX (Ser¹³⁹) *in vitro* and *in vivo*.

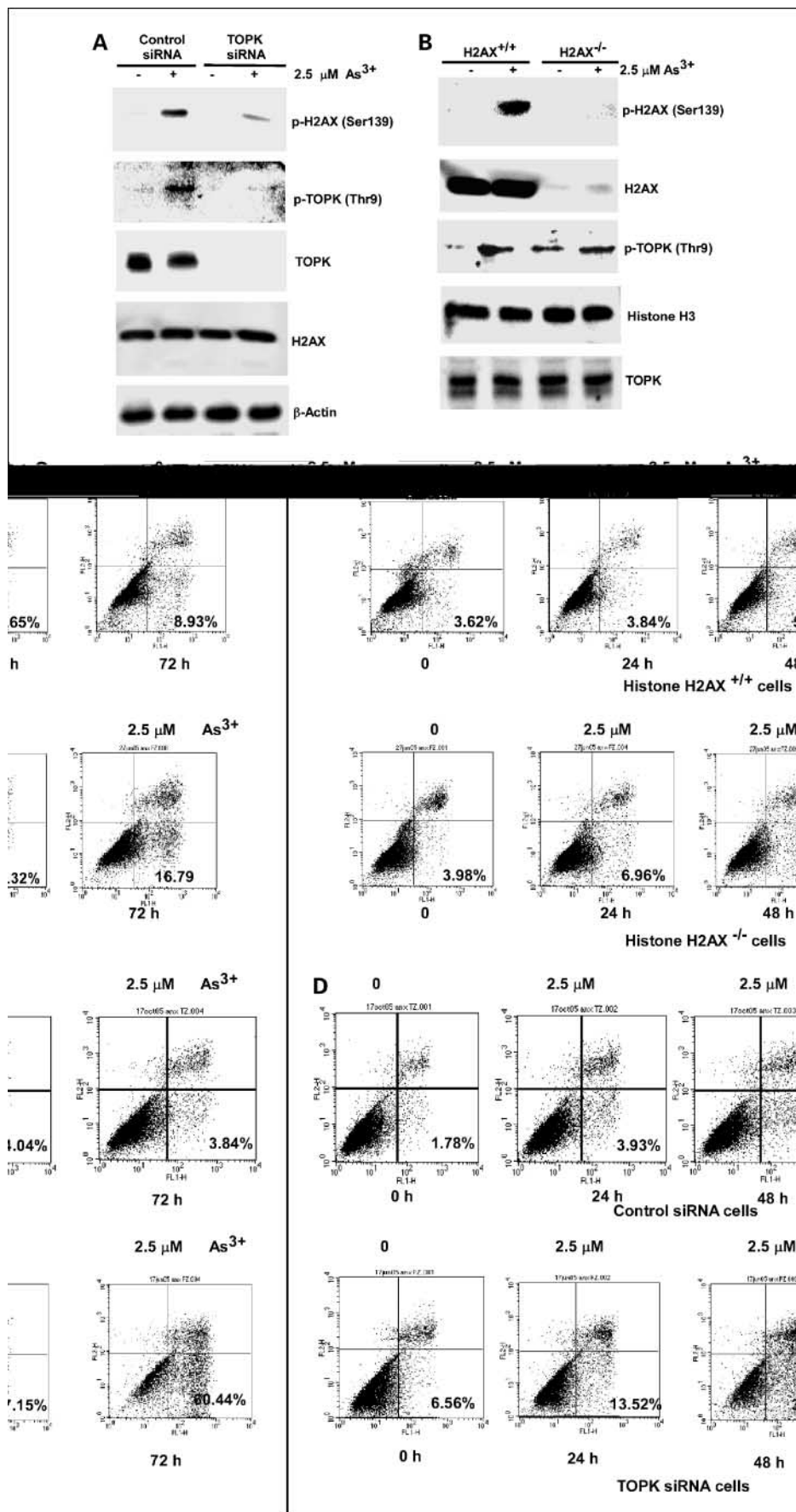


Fig. 5. TOPK inhibits As³⁺-induced apoptosis through phosphorylation of histone H2AX at Ser¹³⁹. *A*, effect of TOPK deficiency on H2AX phosphorylation. Control siRNA and TOPK siRNA cells were cultured and treated with 2.5 μmol/L As³⁺ for 24 hours. Phosphorylation of histone H2AX at Ser¹³⁹ and TOPK at Thr⁹ was visualized by Western blotting using phosphorylated-specific antibodies. Total TOPK, H2AX, and β-actin were used as internal controls for confirmation of TOPK deficiency and equal protein loading. *B*, As³⁺ induced phosphorylation of H2AX in H2AX^{+/+} cells but had no effect on phosphorylation of TOPK in H2AX^{+/+} or H2AX^{-/-} cells. Total TOPK, H2AX, and histone H3 were used as internal controls for confirmation of H2AX deficiency and equal protein loading. *C*, flow cytometry analysis of apoptosis in H2AX^{+/+} and H2AX^{-/-} cells. *D*, flow cytometry analysis of apoptosis in control siRNA or TOPK siRNA cells. Cells were incubated with Annexin V – conjugated FITC after 24 hours of treatment with 2.5 μmol/L As³⁺. Stained cells were analyzed by flow cytometry. Bottom right, percentage of early apoptotic cells (Annexin V – stained positive cells). These data are representative of at least four independent experiments.

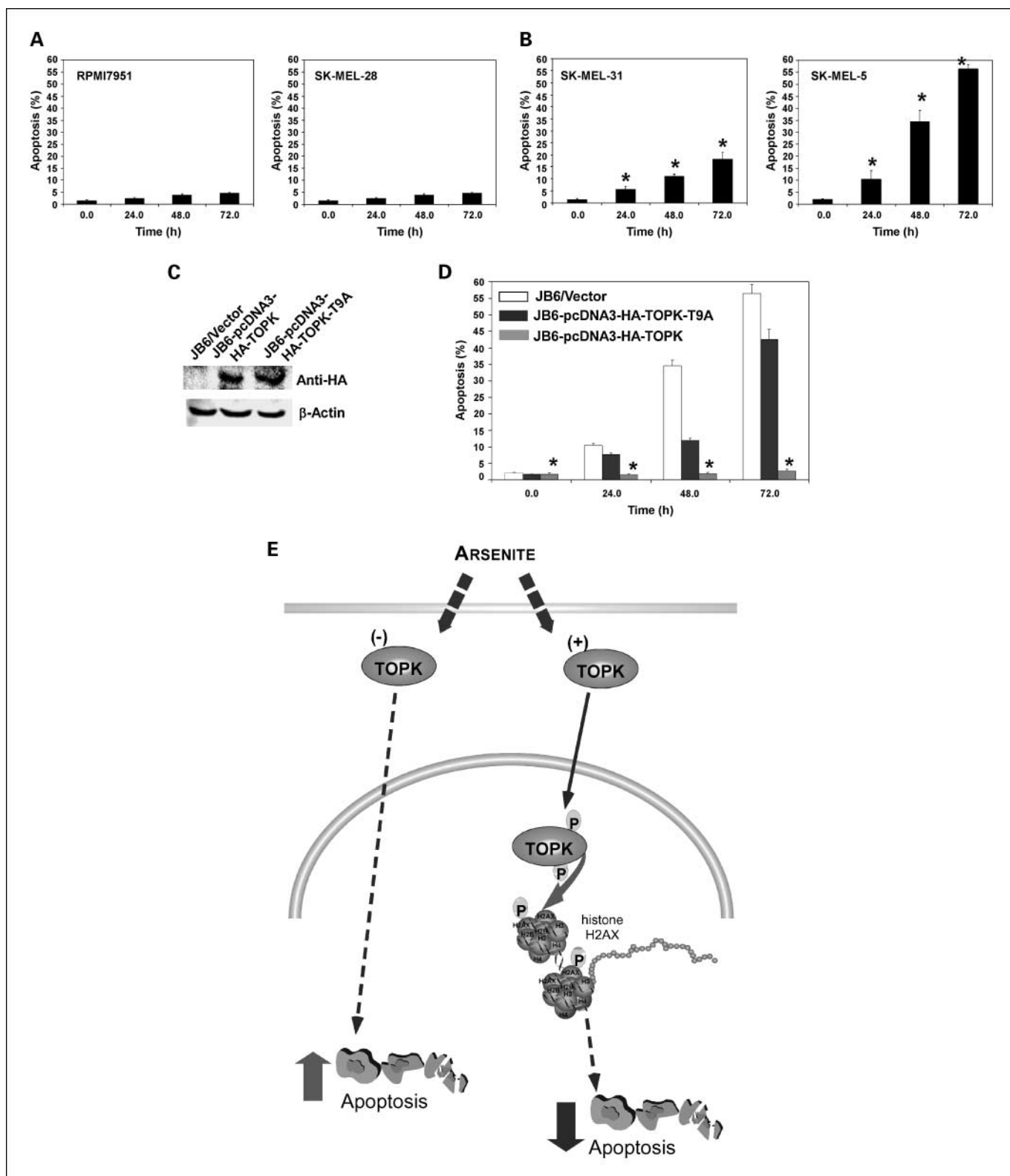


Fig. 6. TOPK blocks As^{3+} -induced apoptosis in RPMI7951 melanoma cells. **A**, As^{3+} does not induce apoptosis in cell lines that express TOPK compared (**B**) with cell lines that do not express TOPK. Columns, mean of four independent experiments; bars, SD. *, $P < 0.0001$, significant increase in apoptosis over time. **C**, JB6 cells were transfected with pcDNA3-HA-TOPK (*JB6-pcDNA3-HA-TOPK*), pcDNA3-HA-TOPK-T9A mutant (*JB6-pcDNA3-HA-TOPK-T9A*), or mock vector (*JB6/Vector*). Expression of HA-TOPK was detected with a HA antibody; β -actin was used as an internal control to verify equal protein loading. **D**, apoptosis is not induced in JB6 cells overexpressing TOPK but is restored in cells expressing mutant TOPK. JB6 cells were transfected as in (**C**) and cultured for 24, 48, or 72 hours with $2.5 \mu\text{M}$ As^{3+} . Apoptosis was determined by flow cytometry using Annexin V – conjugated FITC. Columns, mean of at least four independent experiments; bars, SD. *, $P < 0.0001$, significantly less apoptosis in JB6-TOPK-overexpressing cells compared with either JB6/Vector or JB6-TOPK-T9A mutant cells. **E**, in cells expressing TOPK and stimulated with As^{3+} , TOPK is localized in the nucleus, where it phosphorylates histone H2AX resulting in decreased induction of apoptosis.

Further, Western blot and immunocytofluorescence analyses clearly showed that As³⁺ induced the accumulation of phosphorylated TOPK and phosphorylated H2AX in the nucleus of RPMI7951 cells. Another group has also shown that arsenic treatment induces the phosphorylation and nuclear accumulation of histone H2AX (28). However, our data indicated the colocalization and direct involvement of TOPK in As³⁺-induced apoptosis. The accumulation of phosphorylated H2AX in the nucleus suggested that DNA damage occurred in As³⁺-treated RPMI7951 cells. Previous data showed that, after γ -irradiation, nuclei from H2AX^{+/+} and H2AX^{-/-} fibroblasts exhibited 0.25% and 10% nuclear fragmentation, respectively (17). Loss of H2AX has been shown to lead to increased chromosomal abnormalities, deficiencies in gene targeting, and radiation sensitivity. Furthermore, DNA repair was observed to proceed less efficiently in the absence of H2AX, resulting in increased apoptosis (17). In the present study, we showed that apoptosis in H2AX^{-/-} cells was increased substantially compared with H2AX^{+/+} cells, and in TOPK siRNA-transfected cells, As³⁺-induced apoptosis was also markedly increased. These results suggested that TOPK phosphorylation of histone H2AX is associated with an inhibition of As³⁺-induced apoptosis in RPMI7951 melanoma cells.

Investigations using many different experimental systems suggested that arsenic may offer significant therapeutic benefits to patients across many neoplasms, and numerous clinical trials are under way in hematopoietic malignancies and solid tumors. Miller et al. (37) summarized reports of the activity of arsenic in animal models and in the clinic. Low doses of arsenic trioxide (0.06-0.2 mg/kg of body) can induce complete remission in relapsed acute promyelocytic leukemia patients, and complete remissions occurred in 11 of the 12 patients (38). Low doses of As³⁺ induced apoptosis in some (11, 32–34), but not all, cancer cell types (39–41), suggesting that a mechanism exists that is responsible for resistance to As³⁺. Using different

melanoma cell lines with different levels of TOPK expression, we found that As³⁺ induces apoptosis dependent on TOPK expression level. In melanoma cells without expression of TOPK, a low concentration of As³⁺ induces rapid apoptosis—more than 25% to 50% in 48 hours. In contrast, melanoma cells expressing high levels of TOPK showed full resistance to As³⁺ following 72 hours of exposure, suggesting that melanoma cell lines expressing TOPK are more resistant to As³⁺-induced apoptosis. These various melanoma cells also display other abnormalities. For example, the *p16* gene is deleted in SK-MEL5 (42) cells. Furthermore, *B-raf* is mutated (V599E) in SK-MEL28 and SK-MEL5 cells but not in SK-MEL31 cells (43, 44). Interestingly, the TOPK-expressing SK-MEL28 and RPMI7951 cells each express a mutant *p53* (45, 46), whereas SK-MEL5 cells express wild-type *p53* (45). However, additional studies are needed to specifically link the genetic background of these cell lines with resistance to As³⁺-induced apoptosis. Our study indicated that this resistance seems to be related to the activation and phosphorylation of histone H2AX by activated TOPK (Fig. 6E). In this model, cells lacking TOPK expression readily undergo apoptosis induced by low levels of As³⁺. On the other hand, in cells expressing TOPK, As³⁺ induces its phosphorylation, which leads to phosphorylation of histone H2AX and resistance to apoptosis. Thus, discovery of a small-molecule inhibitor of TOPK may be very important in combination with low doses of As³⁺ in the treatment of melanomas and other TOPK-positive cancers.

Acknowledgments

We thank Dr. Andre Nussenzweig for the H2AX^{+/+} and H2AX^{-/-} murine embryonic fibroblasts, Dr. J. Abe for pcDNA3-HA-TOPK and pcDNA3-HA-TOPK-T9A, Todd Schuster for flow cytometry analysis, Andria Hansen for secretarial assistance, and Paul Hoversten for his help in the writing of the text for this article.

References

- Abe Y, Matsumoto S, Kito K, Ueda N. Cloning and expression of a novel MAPKK-like protein kinase, lymphokine-activated killer T-cell-originated protein kinase, specifically expressed in the testis and activated lymphoid cells. *J Biol Chem* 2000;275:21525–31.
- Gaudet S, Branton D, Lue RA. Characterization of PDZ-binding kinase, a mitotic kinase. *Proc Natl Acad Sci U S A* 2000;97:5167–72.
- Simons-Evelyn M, Bailey-Dell K, Toretsky JA, et al. PBK/TOPK is a novel mitotic kinase which is upregulated in Burkitt's lymphoma and other highly proliferative malignant cells. *Blood Cells Mol Dis* 2001;27:825–9.
- Cote S, Simard C, Lemieux R. Regulation of growth-related genes by interleukin-6 in murine myeloma cells. *Cytokine* 2002;20:113–20.
- Yuryev A, Wennogle LP. Novel raf kinase protein-protein interactions found by an exhaustive yeast two-hybrid analysis. *Genomics* 2003;81:112–25.
- Matsumoto S, Abe Y, Fujibuchi T, et al. Characterization of a MAPKK-like protein kinase TOPK. *Biochem Biophys Res Commun* 2004;325:997–1004.
- Nandi A, Rapoport AP. Expression of PDZ-binding kinase (PBK) is regulated by cell cycle-specific transcription factors E2F and CREB/ATF. *Leuk Res* 2005;96:271–8.
- Qian Y, Castranova V, Shi X. New perspectives in arsenic-induced cell signal transduction. *J Inorg Biochem* 2003;96:271–8.
- Dong Z. The molecular mechanisms of arsenic-induced cell transformation and apoptosis. *Environ Health Perspect* 2002;110 Suppl 5:757–9.
- Zhu XH, Shen YL, Jing YK, et al. Apoptosis and growth inhibition in malignant lymphocytes after treatment with arsenic trioxide at clinically achievable concentrations. *J Natl Cancer Inst* 1999;91:772–8.
- Ivanov VN, Hei TK. Arsenite sensitizes human melanomas to apoptosis via tumor necrosis factor α -mediated pathway. *J Biol Chem* 2004;279:22747–58.
- Ling YH, Jiang JD, Holland JF, Perez-Soler R. Arsenic trioxide produces polymerization of microtubules and mitotic arrest before apoptosis in human tumor cell lines. *Mol Pharmacol* 2002;62:529–38.
- Clark WH, Jr., Elder DE, Guerry D 4th, Epstein MN, Greene MH, Van Horn M. A study of tumor progression: the precursor lesions of superficial spreading and nodular melanoma. *Hum Pathol* 1984;15:1147–65.
- Warters RL, Adamson PJ, Pond CD, Leachman SA. Melanoma cells express elevated levels of phosphorylated histone H2AX foci. *J Invest Dermatol* 2005;124:807–17.
- Bassing CH, Suh H, Ferguson DO, et al. Histone H2AX: a dosage-dependent suppressor of oncogenic translocations and tumors. *Cell* 2003;114:359–70.
- Celeste A, Difilippantonio S, Difilippantonio MJ, et al. H2AX haploinsufficiency modifies genomic stability and tumor susceptibility. *Cell* 2003;114:371–83.
- Celeste A, Petersen S, Romanienko PJ, et al. Genomic instability in mice lacking histone H2AX. *Science* 2002;296:922–7.
- Elbashir SM, Harborth J, Lendeckel W, et al. Duplexes of 21-nucleotide RNAs mediate RNA interference in cultured mammalian cells. *Nature* 2001;411:494–8.
- Moseley MA, Deterding LJ, Tomer KB, Jorgenson JW. Nanoscale packed-capillary liquid chromatography coupled with mass spectrometry using a coaxial continuous-flow fast atom bombardment interface. *Anal Chem* 1991;63:1467–73.
- Gatlin CL, Kleemann GR, Hays LG, Link AJ, Yates JR III. Protein identification at the low femtomole level from silver-stained gels using a new fritless electrospray interface for liquid chromatography-microspray and nanospray mass spectrometry. *Anal Biochem* 1998;263:93–101.
- Tang WH, Halpern BR, Shilov IV, et al. Discovering known and unanticipated protein modifications using MS/MS database searching. *Anal Chem* 2005;77:3931–46.
- Bradford MM. A rapid and sensitive method for the quantitation of microgram quantities of protein utilizing the principle of protein-dye binding. *Anal Biochem* 1976;72:248–54.
- Ward IM, Chen J. Histone H2AX is phosphorylated in an ATR-dependent manner in response to replicational stress. *J Biol Chem* 2001;276:47759–62.
- Biemann K. Contributions of mass spectrometry to peptide and protein structure. *Biomed Environ Mass Spectrom* 1988;16:99–111.
- Redon C, Pilch D, Rogakou E, et al. Histone H2A variants H2AX and H2AZ. *Curr Opin Genet Dev* 2002;12:162–9.

26. Fernandez-Capetillo O, Lee A, Nussenzweig M, Nussenzweig A. H2AX: the histone guardian of the genome. *DNA Repair (Amst)* 2004;3:959–67.
27. Lu C, Zhu F, Cho Y-Y, et al. Cell apoptosis: requirement of H2AX in DNA ladder formation, but not for the action of caspase-3. *Mol Cell* 2006;23:121–32.
28. Yih LH, Hsueh SW, Luu WS, Chiu TH, Lee TC. Arsenite induces prominent mitotic arrest via inhibition of G₂ checkpoint activation in CGL-2 cells. *Carcinogenesis* 2005;26:53–63.
29. Nandi A, Tidwell M, Karp J, Rapoport AP. Protein expression of PDZ-binding kinase is up-regulated in hematologic malignancies and strongly down-regulated during terminal differentiation of HL-60 leukemic cells. *Blood Cells Mol Dis* 2004;32:240–5.
30. Daniel R, Ramcharan J, Rogakou E, et al. Histone H2AX is phosphorylated at sites of retroviral DNA integration but is dispensable for postintegration repair. *J Biol Chem* 2004;279:45810–4.
31. Wang TS, Hsu TY, Chung CH, et al. Arsenite induces oxidative DNA adducts and DNA-protein cross-links in mammalian cells. *Free Radic Biol Med* 2001;31:321–30.
32. Schwerdtle T, Walter I, Mackiw I, Hartwig A. Induction of oxidative DNA damage by arsenite and its trivalent and pentavalent methylated metabolites in cultured human cells and isolated DNA. *Carcinogenesis* 2003;24:967–74.
33. Bode AM, Dong Z. The paradox of arsenic: molecular mechanisms of cell transformation and chemotherapeutic effects. *Crit Rev Oncol Hematol* 2002;42:5–24.
34. Bode A, Dong Z. Apoptosis induction by arsenic: mechanisms of action and possible clinical applications for treating therapy-resistant cancers. *Drug Resist Updat* 2000;3:21–9.
35. Alemany M, Levin J. The effects of arsenic trioxide (As₂O₃) on human megakaryocytic leukemia cell lines. With a comparison of its effects on other cell lineages. *Leuk Lymphoma* 2000;38:153–63.
36. Rousselot P, Labaume S, Marolleau JP, et al. Arsenic trioxide and melarsoprol induce apoptosis in plasma cell lines and in plasma cells from myeloma patients. *Cancer Res* 1999;59:1041–8.
37. Miller WH, Jr., Schipper HM, Lee JS, Singer J, Waxman S. Mechanisms of action of arsenic trioxide. *Cancer Res* 2002;62:3893–903.
38. Soignet SL, Frankel SR, Douer D, et al. United States multicenter study of arsenic trioxide in relapsed acute promyelocytic leukemia. *J Clin Oncol* 2001;19:3852–60.
39. Yang CH, Kuo ML, Chen JC, Chen YC. Arsenic trioxide sensitivity is associated with low level of glutathione in cancer cells. *Br J Cancer* 1999;81:796–9.
40. Gianni M, Koken MH, Chelbi-Alix MK, et al. Combined arsenic and retinoic acid treatment enhances differentiation and apoptosis in arsenic-resistant NB4 cells. *Blood* 1998;91:4300–10.
41. Munshi NC. Arsenic trioxide: an emerging therapy for multiple myeloma. *Oncologist* 2001;6 Suppl 2:17–21.
42. Berggren P, Kumar R, Sakano S, et al. Detecting homozygous deletions in the CDKN2A(p16(INK4a))/ARF(p14(ARF)) gene in urinary bladder cancer using real-time quantitative PCR. *Clin Cancer Res* 2003;9:235–42.
43. Davies H, Bignell GR, Cox C, et al. Mutations of the BRAF gene in human cancer. *Nature* 2002;417:949–54.
44. Grbovic OM, Basso AD, Sawai A, et al. V600E B-Raf requires the Hsp90 chaperone for stability and is degraded in response to Hsp90 inhibitors. *Proc Natl Acad Sci U S A* 2006;103:57–62.
45. Girnita L, Girnita A, Larsson O. Mdm2-dependent ubiquitination and degradation of the insulin-like growth factor 1 receptor. *Proc Natl Acad Sci U S A* 2003;100:8247–52.
46. Haapajarvi T, Pitkanen K, Laiho M. Human melanoma cell line UV responses show independency of p53 function. *Cell Growth Differ* 1999;10:163–71.